



UNIVERSITÀ
DI SIENA
1240

Highlights on the first 8 years of CALET experiment observations on the International Space Station

Caterina Checchia

University of Siena

On behalf of the CALET collaboration

XIX Vulcano Workshop 2024 - Frontier Objects in Astrophysics and Particle Physics

28/05/2024 – 01/06/2024 Ischia (Napoli)

CALET collaboration members

O. Adriani,^{1, 2} Y. Akaike,^{3, 4} K. Asano,⁵ Y. Asaoka,⁵ E. Berti,¹ G. Bigongiari,^{6, 7} W.R. Binns,⁸ M. Bongi,^{1, 2} P. Brogi,^{6, 7} A. Bruno,⁹ J.H. Buckley,⁸ N. Cannady,^{10, 11, 12} G. Castellini,¹³ C. Checchia,^{6, 7} M.L. Cherry,¹⁴ G. Collazuol,^{15, 16} G.A. de Nolfo,⁹ K. Ebisawa,¹⁷ A. W. Ficklin,¹⁴ H. Fuke,¹⁷ S. Gonzi,^{1, 2} T.G. Guzik,¹⁴ T. Hams,¹⁰ K. Hibino,¹⁸ M. Ichimura,¹⁹ K. Ioka,²⁰ W. Ishizaki,⁵ M.H. Israel,⁸ K. Kasahara,²¹ J. Kataoka,²² R. Kataoka,²³ Y. Katayose,²⁴ C. Kato,²⁵ N. Kawanaka,²⁰ Y. Kawakubo,¹⁴ K. Kobayashi,^{3, 4} K. Kohri,²⁶ H.S. Krawczynski,⁸ J.F. Krizmanic,¹¹ P. Maestro,^{6,} P.S. Marrocchesi,^{6, 7} A.M. Messineo,^{27, 7} J.W. Mitchell,¹¹ S. Miyake,²⁸ A.A. Moiseev,^{29, 11, 12} M. Mori,³⁰ N. Mori,² H.M. Motz,³¹ K. Munakata,²⁵ S. Nakahira,¹⁷ J. Nishimura,¹⁷ S. Okuno,¹⁸ J.F. Ormes,³² S. Ozawa,³³ L. Pacini,^{1, 2, 13} P. Papini,² B.F. Rauch,⁸ S.B. Ricciarini,^{13, 2} K. Sakai,^{10, 11, 12} T. Sakamoto,³⁴ M. Sasaki,^{29, 11, 12} Y. Shimizu,¹⁸ A. Shiomi,³⁵ P. Spillantini,¹ F. Stolzi,^{6, 7} S. Sugita,³⁴ A. Sulaj,^{6, 7} M. Takita,⁵ T. Tamura,¹⁸ T. Terasawa,⁵ S. Torii,³ Y. Tsunesada,^{36, 37} Y. Uchihori,³⁸ E. Vannuccini,² J.P. Wefel,¹⁴ K. Yamaoka,³⁹ S. Yanagita,⁴⁰ A. Yoshida,³³ K. Yoshida,²¹ and W. V. Zober⁸

1) University of Florence, Italy

2) INFN Florence, Italy

3) WISE, Waseda University, Japan

4) JEM Utilization Center, JAXA, Japan

5) ICRR, University of Tokyo, Japan

6) University of Siena, Italy

7) INFN Pisa, Italy

8) Washington University, St. Louis, USA

9) Heliospheric Physics Laboratory, NASA/GSFC, USA

10) University of Maryland, Baltimore County, USA

11) Astroparticle Physics Laboratory, NASA/GSFC, USA

12) CRESST, NASA/GSFC, USA

13) IFAC, CNR, Italy

14) Louisiana State University, USA

15) University of Padova, Italy

16) INFN Padova, Italy

17) ISAS, JAXA, Japan

18) Kanagawa University, Japan

19) Hirosaki University, Japan

20) YITP, Kyoto University, Japan

21) Shibaura Institute of Technology, Japan

22) ASE, Waseda University, Japan

23) NIPR, Japan

24) Yokohama National University, Japan

25) Shinshu University, Japan

26) IPNS, KEK, Japan

27) University of Pisa

28) NIT(KOSEN), Ibaraki College, Japan

29) University of Maryland, College Park, USA

30) Ritsumeikan University, Japan

31) GCSE, Waseda University, Japan

32) University of Denver, USA

33) NICT, Japan

34) Aoyama Gakuin University, Japan

35) Nihon University, Japan

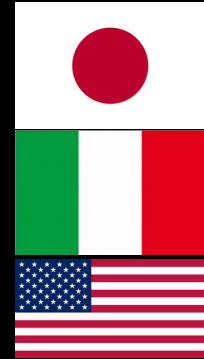
36) Osaka Metropolitan University, Japan

37) NITEP, Osaka Metropolitan University, Japan

38) QST, Japan

39) Nagoya University, Japan

40) Ibaraki University, Japan



PI: Japan
Co-PI: Italy
Co-PI: USA



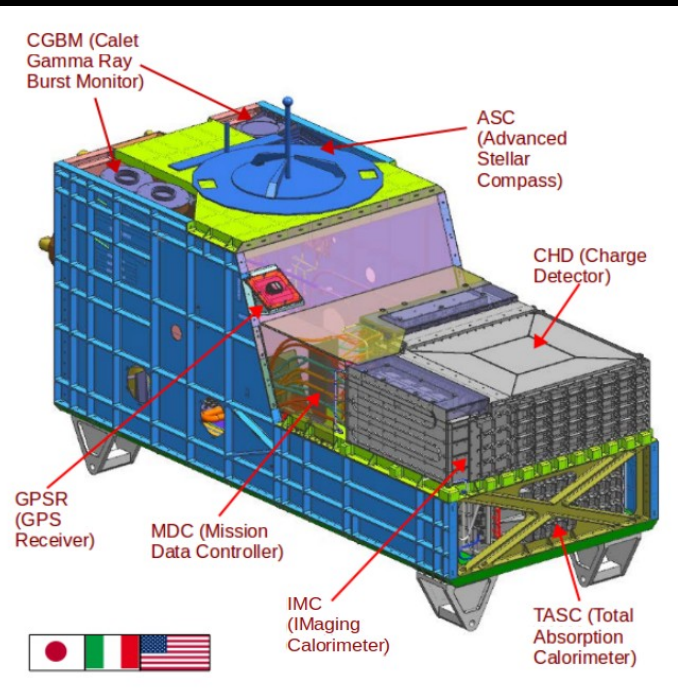
CALET payload

CALET launch on Aug. 19th, 2015 on Japanese H2-B rocket



CALET was emplaced on JEM-EF port#9 on Aug. 25th, 2015

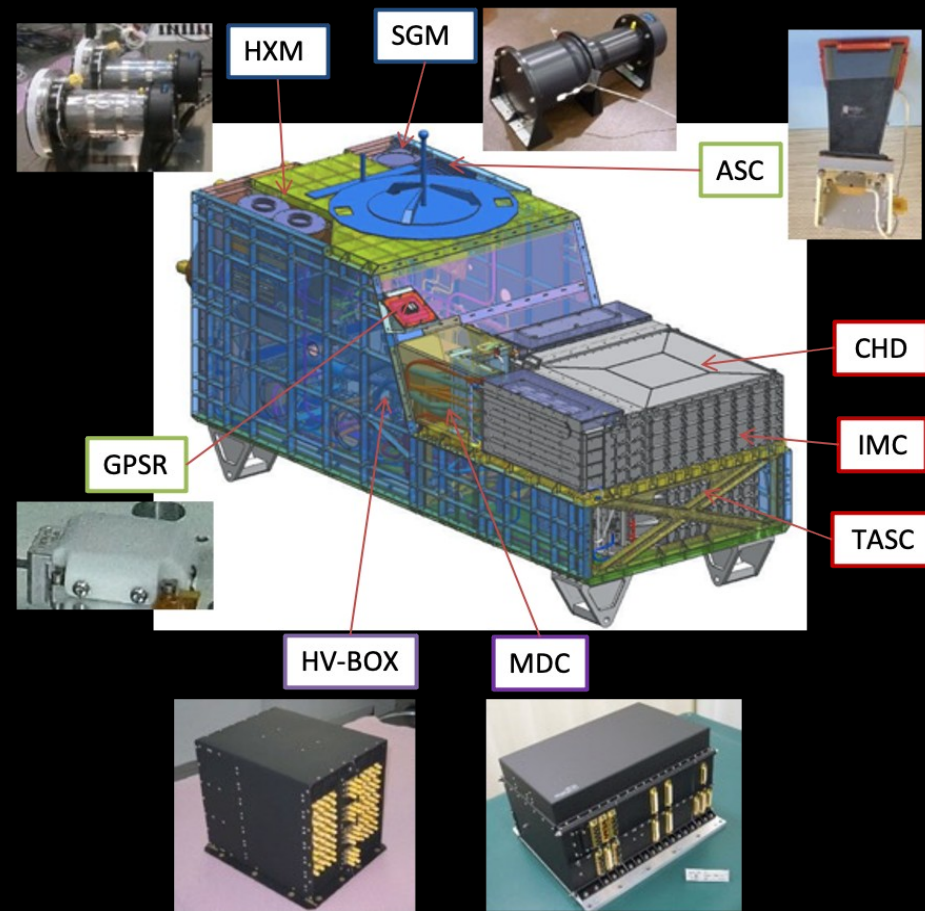
JEM-EF
Port#9



- JEM Standard Payload
- Mass: 612.8 kg
- Size: 1850 mm (L) x 800 mm (W) x 1000 mm (H)
- Power Consumption: 507 W (max)
- Telemetry: Medium (Low) 600 (50) kbps (6.5 GB/day)

CALET started scientific observations on Oct. 13th, 2015
More than 4.5 billion events collected so far.

Overview of the CALET payload



CAL:

- Charge Detector (CHD)
- Imaging Calorimeter (IMC)
- Total Absorption Calorimeter (TASC)

CGBM (CALET Gamma Ray Burst Monitor)

- Hard X-ray Monitor (HXM) x 2 (3 sr)
Scintillators LaBr_3 : 7 keV \sim 1 MeV
- Soft γ -ray Monitor (SGM) (8 sr)
Scintillators BGO: 40keV \sim 20MeV

Data Processing & Power Supply:

- Mission Data Controller (MDC)
CPU, telemetry, power, trigger etc.
- HV-BOX (Italian contribution)
HV supply (PMT: 68ch, APD: 22ch)

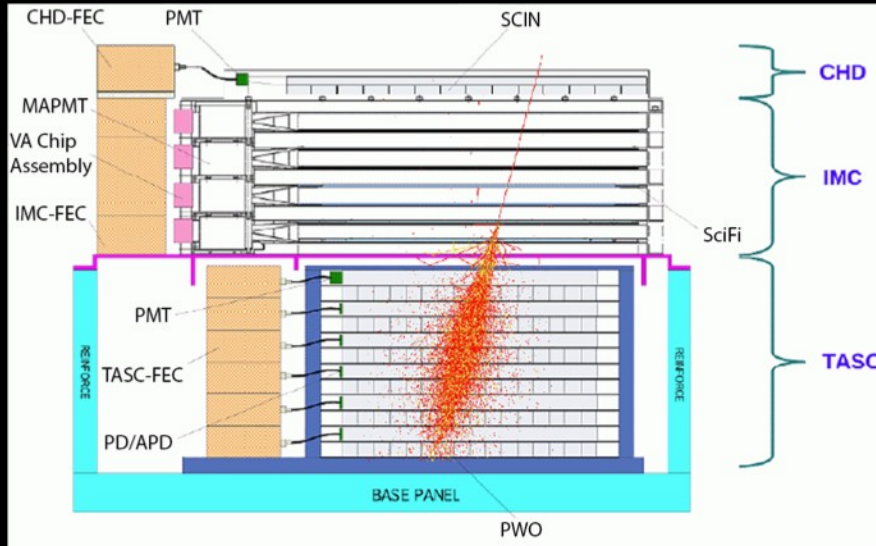
Support Sensors

- Advanced Stellar Compass (ASC)
Directional measurement
- GPS Receiver (GPSR)
Time stamp of triggered event (<1ms)

CALET Instrument

Field Of View: $\sim 45^\circ$ from Zenith
Geometrical Factor: $\sim 1040 \text{ cm}^2\text{sr}$ (for e^-)
Total thickness: $30 X_0$ ($1.3 \lambda_I$)

A 30 radiation length deep calorimeter designed to detect electrons and gammas up to 20 TeV and cosmic rays up to 1 PeV



CHD (Charge Detector)

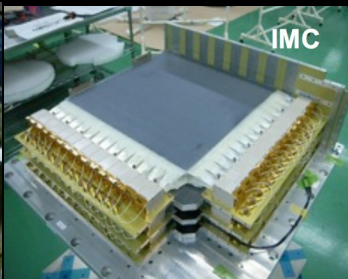
- 14x2 plastic scintillator paddles
- Single element charge ID from p to Fe and above ($Z = 40$)
- Charge resolution: $0.15 e$ (C), $0.35 e$ (Fe)

IMC (Imaging Calorimeter)

- SciFi belts ($8 \times 2 \times 448, 1 \text{ mm}^2$) + Tungsten plates (7 layers: $3 X_0 = 0.2 X_0 \times 5 + 1.0 X_0 \times 2$)
- Track reconstruction and particle ID (up to $Z = 14$), shower imaging
- Angular resolution: $\sim 0.1^\circ$, Spatial resolution on top CHD: $\sim 200 \mu\text{m}$

TASC (Total Absorption Calorimeter)

- 16 x 12 PWO logs: $27 X_0$ (for e^-), $1.2 \lambda_I$ (for p)
- Energy resolution: $\sim 2\%$ for e^- ($>10 \text{ GeV}$), $\sim 30\text{-}35\%$ for p and nuclei
- e/p separation: $\sim 10^5$



CALET objectives

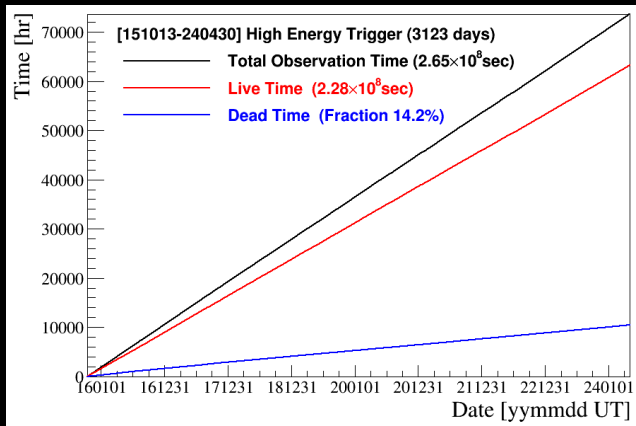
Science objectives	Observation Target	Energy range
Nearby CR sources	Electron Spectrum	100 GeV – 20 TeV
Dark Matter	Signatures in e/γ spectra	100 GeV – 20 TeV
CR origin & acceleration	Electron spectrum P-Fe individual spectra Ultra heavy Ions ($28 < Z \leq 40$)	1 GeV – 20 TeV 10 GeV – 10^3 TeV Few GeV/n
Galactic CR Propagation	B/C sub-Fe/Fe ratios	Up to some TeV/n
Solar Physics	Electron flux	< 10 GeV
Transient Phenomena (GRBs, e.m. counterpart of GW)	Gamma & X-rays	7 keV – 20 MeV

- Wide dynamic range ($1-10^6$ MIP)
- Large thickness ($30 X_0$, $1.3 \lambda_1$)
- Excellent charge ID ($0.2 e^-$)



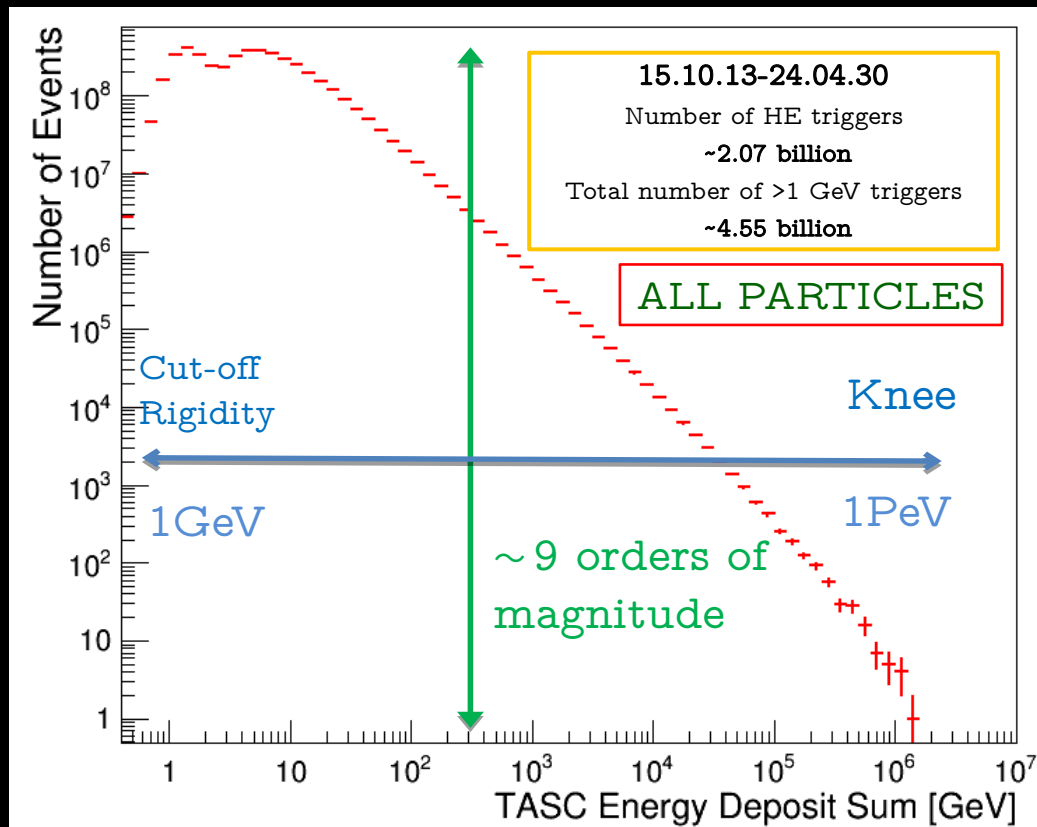
CALET can cover the whole energy range previously investigated in separate subranges by magnetic spectrometers and calorimeters

CALET observation on orbit



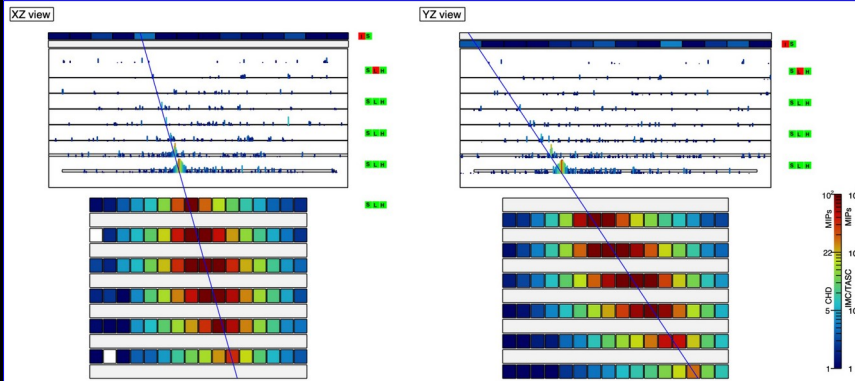
High-energy trigger (> 10 GeV) statistics:

- Operational time 3123 days (> 8 years)^(*)
 - (*) as of Apr. 30, 2024
- Live time fraction $\sim 86\%$
- Exposure of HE trigger $> 275 \text{ m}^2 \text{ sr day}$
- HE-gamma point source exposure $\sim 4.2 \text{ m}^2 \text{ day}$ (for Crab, Geminga)

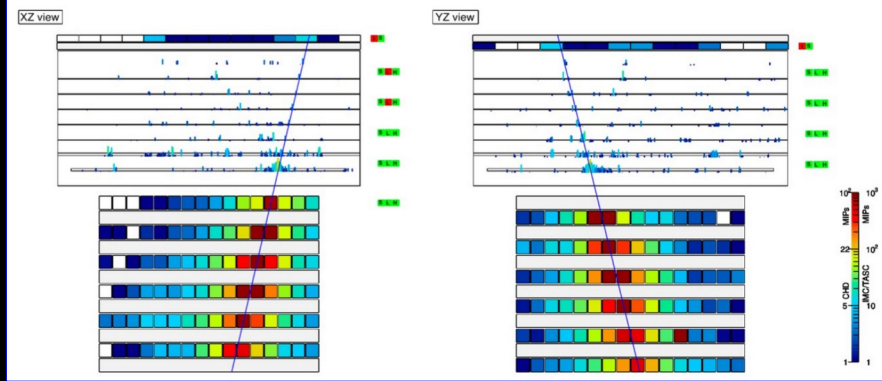


CALET candidates events

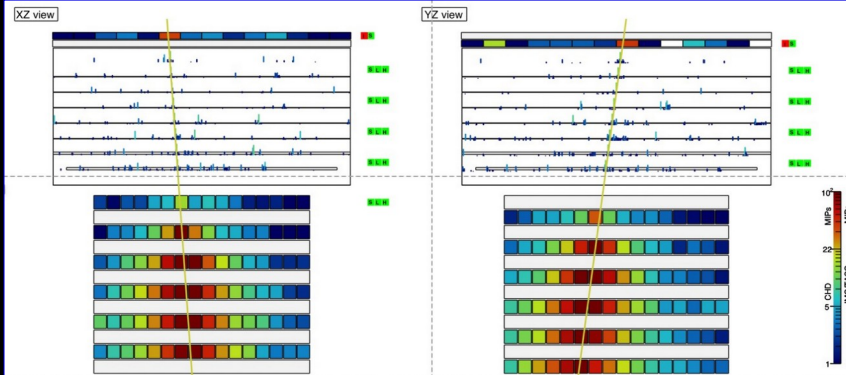
Electron 3 TeV



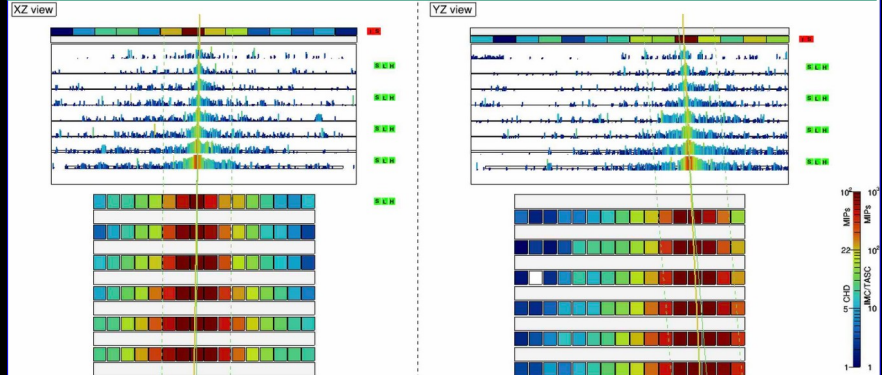
Helium 700 GeV



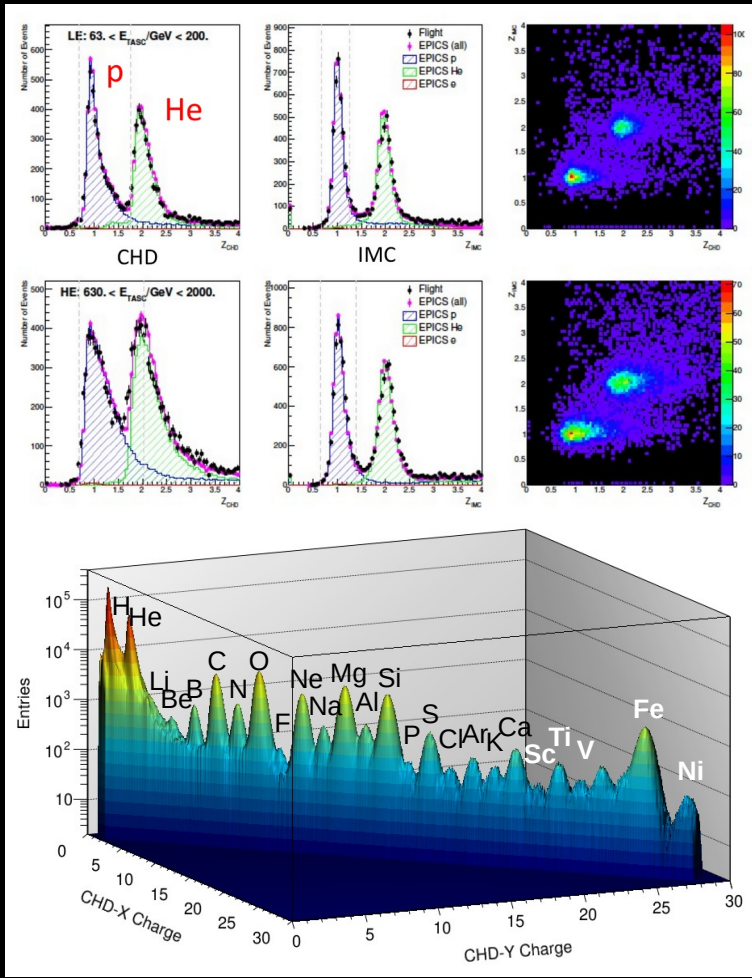
Carbon 2 TeV



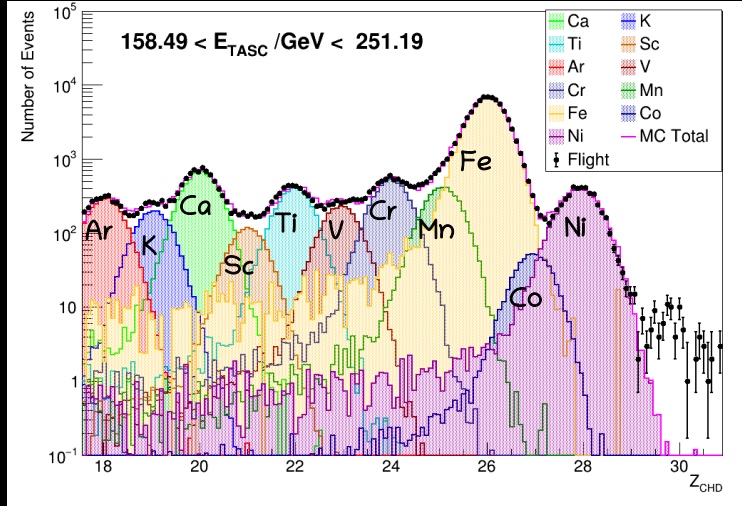
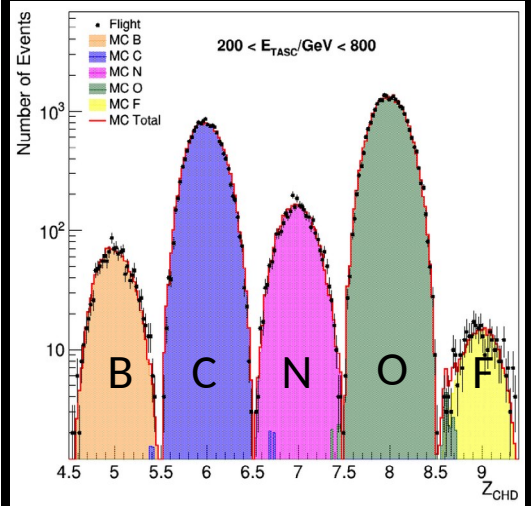
Iron 3.9 TeV



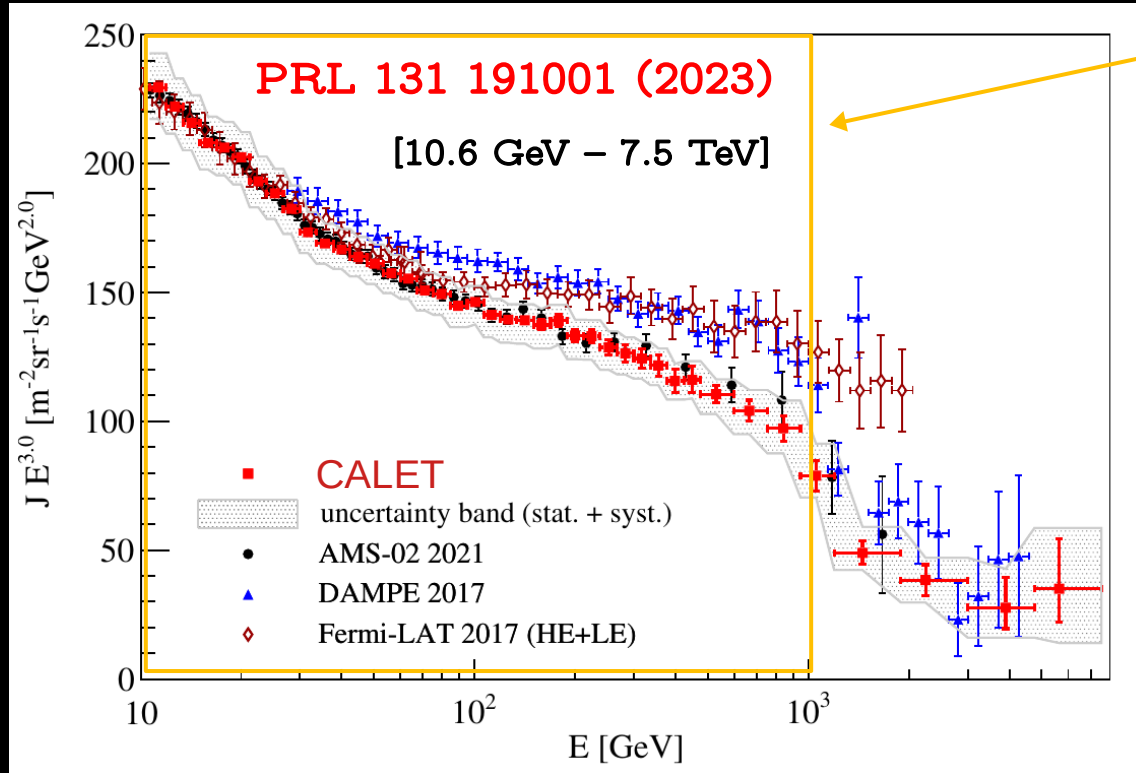
Charge Identification with CALET



- Charge identification for p, He and light nuclei is achieved by CHD+IMC;
- Charge identification for heavy nuclei is achieved by CHD due to saturation of signals occurring in the IMC layers.



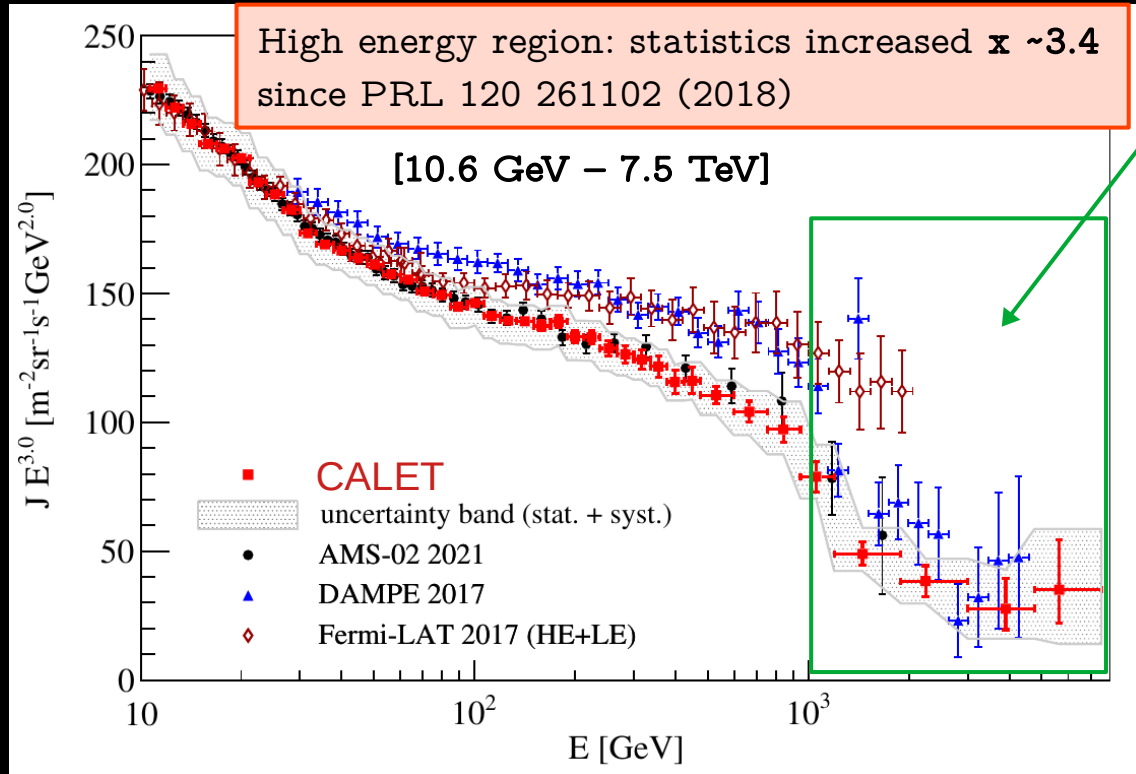
The all electron spectrum



- Up to 2 TeV the **CALET** spectrum is consistent with **AMS02**
- Below 1 TeV present measurements clustered into 2 groups:
 - AMS02 + CALET** and **FERMI+DAMPE** possibly indicating the presence of unknown systematics

Updated spectrum using 2637 days of CALET observations:
Oct. 13, 2015 – Dec. 31, 2022
7.02 million events

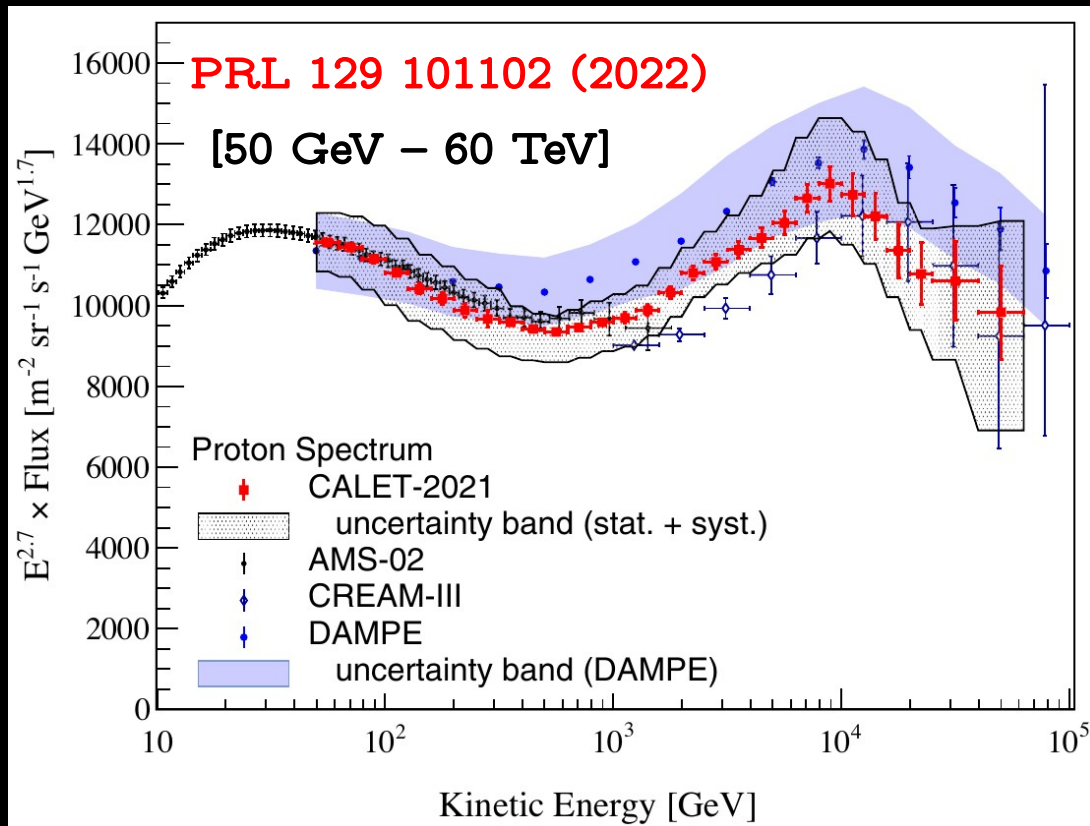
The all electron spectrum



CALET observes a flux suppression above 1 TeV with a **significance of $> 6.5\sigma$** considerable improvement with respect to our previous publication PRL 120 261102 (2018) ($\sim 4\sigma$)

Advanced analysis is ongoing for electron identification above 5 TeV

The proton spectrum

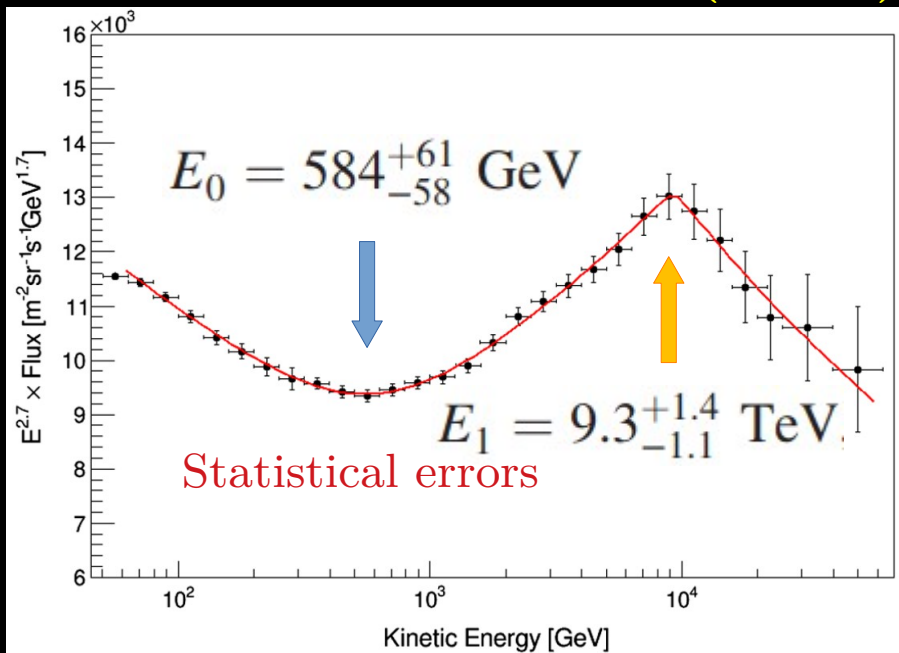


CALET confirms proton spectral hardening above a few hundred GeV with a higher significance of more than 20σ ;

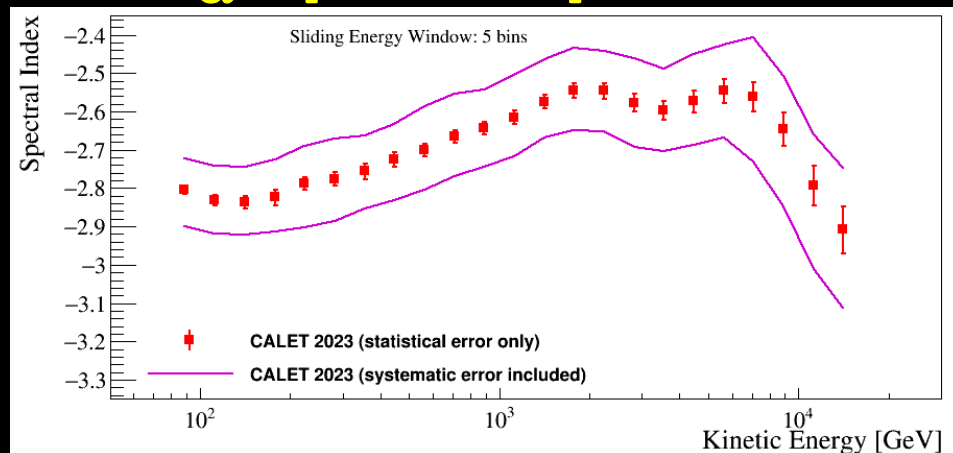
CALET observes a spectral softening starting around 10 TeV consistent, within the errors, with the measurement reported by DAMPE.

The proton spectral index

Fit from 80 GeV to 60 TeV with
Double-Broken Power Law (DBPL)



Energy dependence of spectral index



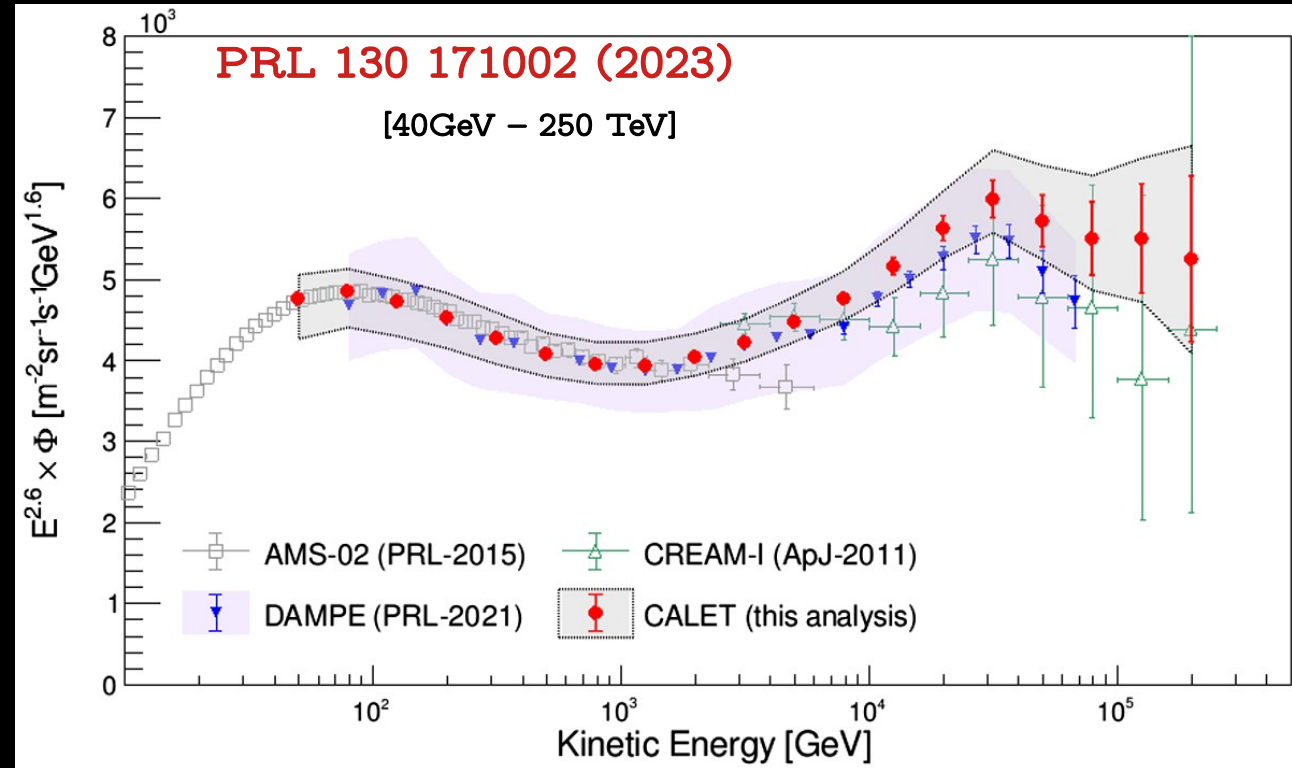
The fit gives a spectral index hardening $\Delta\gamma = 0.28^{+0.04}_{-0.02}$ from $\gamma = -2.83$ and a spectral index softening $\Delta\gamma_1 = -0.34^{+0.06}_{-0.06}$ with $\chi^2/\text{d.o.f.} = 4.4$.

$$\Phi'(E) = E^{2.7} \times C \times \left(\frac{E}{1 \text{ GeV}} \right)^\gamma \times \phi(E)$$

$$\phi(E) = \left[1 + \left(\frac{E}{E_0} \right)^s \right]^{\frac{\Delta\gamma}{s}} \times \left[1 + \left(\frac{E}{E_1} \right)^{s_1} \right]^{\frac{\Delta\gamma_1}{s_1}}$$

Spectral hardening Spectral softening

The helium spectrum

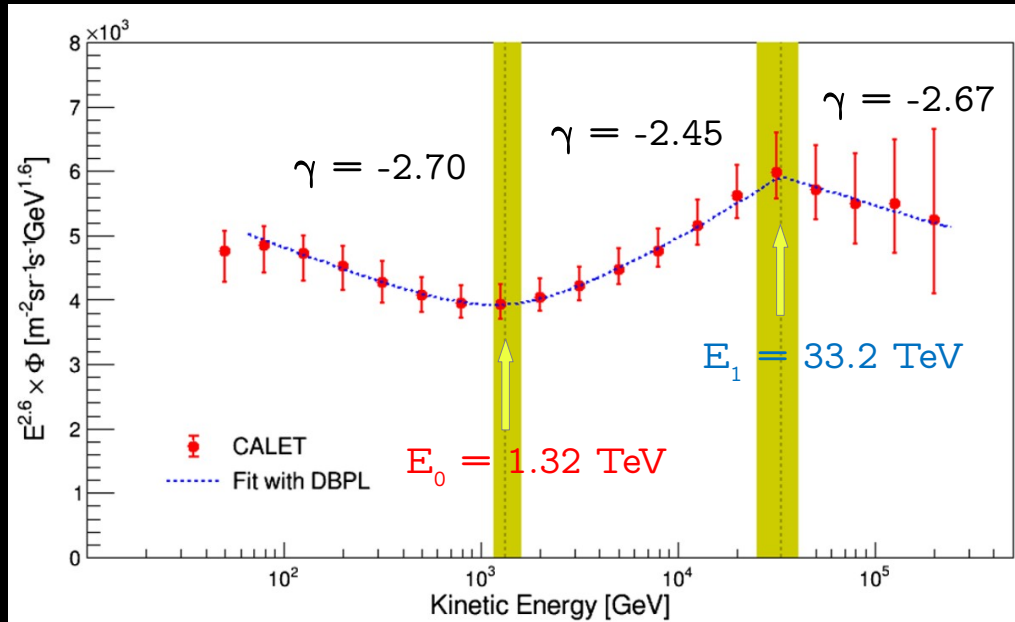


CALET observes spectral **hardening** from a few hundred GeV to a few tens TeV with a significance of **8σ** ;

CALET observes a spectral **softening** starting above few tens of TeV consistent, within the errors, with the measurement reported by DAMPE.

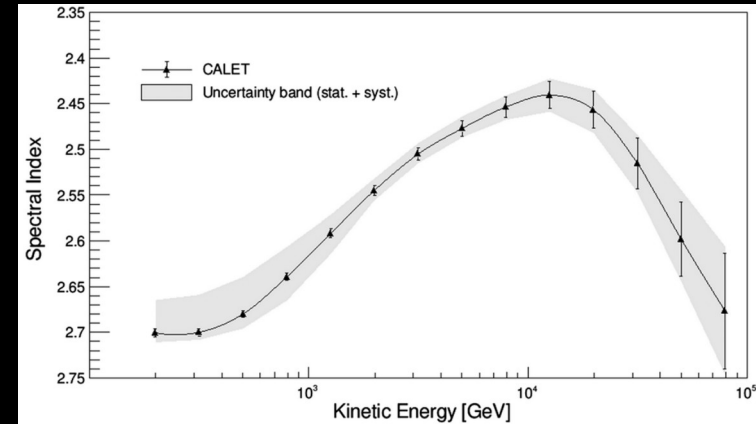
The helium spectral index

Fit with a Double Broken Power Law (DPL)



$$\begin{aligned}
 \gamma &= -2.703^{+0.005}_{-0.006} (\text{stat})^{+0.032}_{-0.009} (\text{syst}); \quad \Delta \gamma = -0.25^{+0.02}_{-0.01} (\text{stat})^{+0.02}_{-0.03} (\text{syst}); \\
 E_0 &= 1319^{+113}_{-93} (\text{stat})^{+267}_{-124} (\text{syst}) \text{ GeV}; \quad S = 2.7^{+0.6}_{-0.5} (\text{stat})^{+3.0}_{-0.9} (\text{syst}); \\
 \Delta \gamma_1 &= -0.22^{+0.07}_{-0.10} (\text{stat})^{+0.03}_{-0.04} (\text{syst}); \quad E_1 = 33.2^{+9.8}_{-6.2} (\text{stat})^{+1.8}_{-2.3} (\text{syst}) \text{ TeV};
 \end{aligned}$$

Energy dependence of spectral index

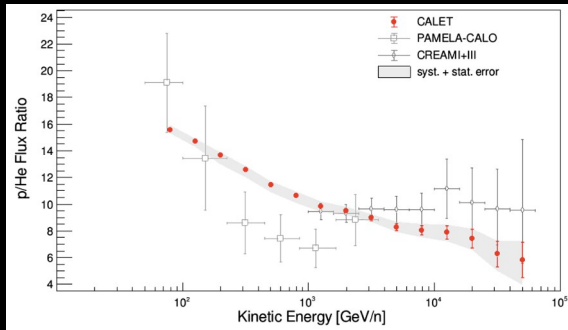
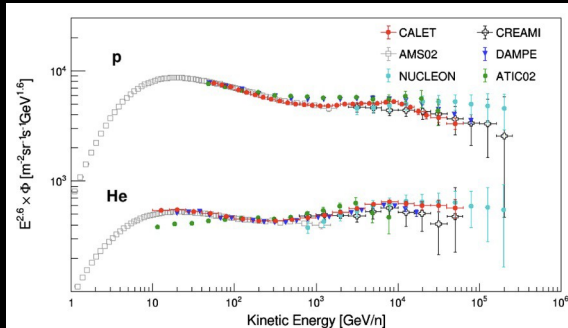


$$\Phi(E) = C \left(\frac{E}{\text{GeV}} \right)^\gamma \left[1 + \left(\frac{E}{E_0} \right)^S \right]^{\frac{\Delta \gamma}{S}} \left[1 + \left(\frac{E}{E_1} \right)^{S_1} \right]^{\frac{\Delta \gamma_1}{S_1}}$$

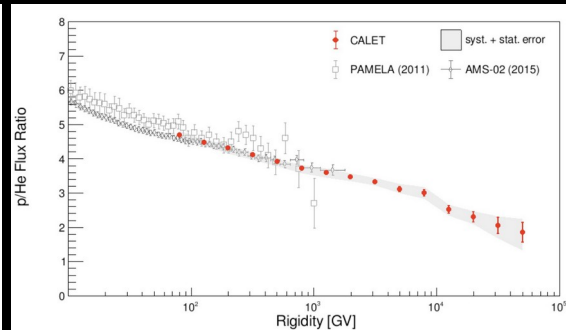
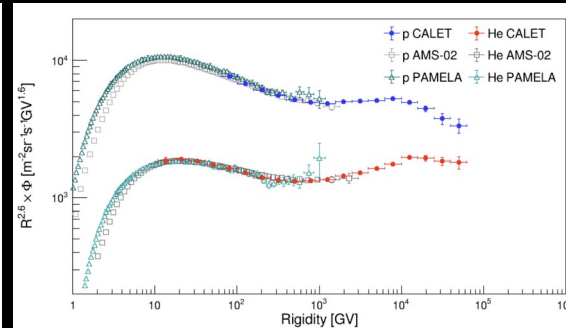
HARDENING SOFTENING

Proton & helium in comparison

Kinetic Energy per Nucleon



Rigidity

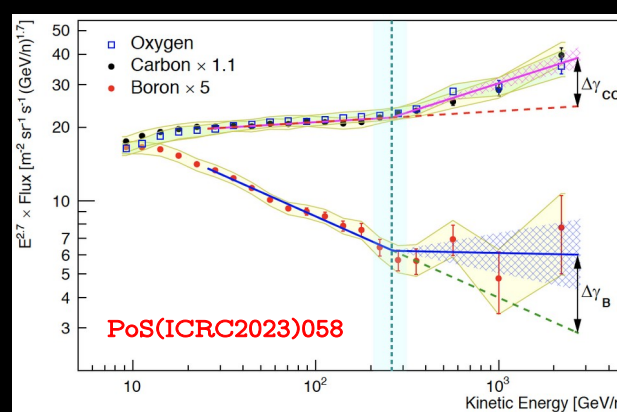
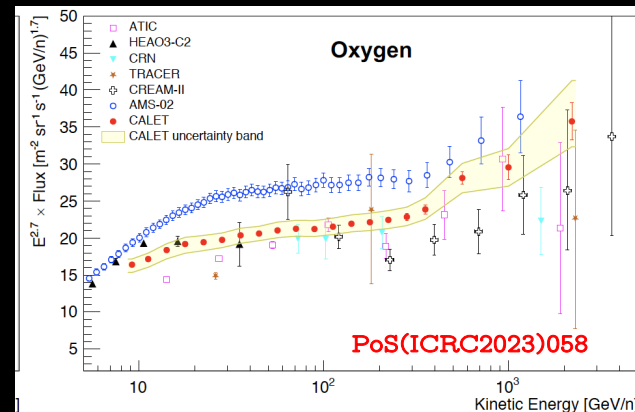
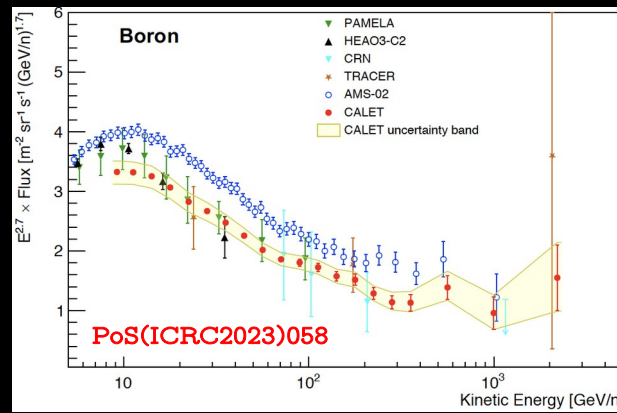
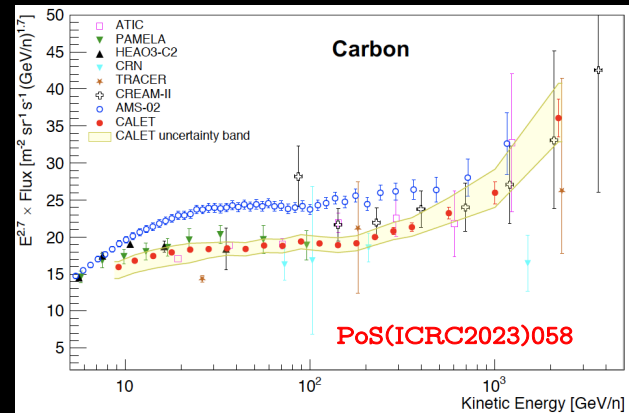


Both proton and helium spectra have a similar structure of **hardening** and **softening** around same region of rigidities.

The softening of p & He spectra around 10 TV indicates a possible relation to the energy limit of shock wave acceleration in SNR.

The spectral index of helium is harder than that of proton (by ~ 0.1) in the whole rigidity range. Possible change of the spectral index of p/He ratio seen above 10 TV will be carefully checked by analyzing higher energy statistics data in the future.

Carbon & Oxygen & Boron spectra



C and O fluxes harden in a similar way above 200 GeV/n.

B spectrum clearly different from C-O as expected for primary and secondary CR. The flux hardens more for B than for C and O above 200 GeV/n, albeit with low statistical significance.

C-O fit

$$\gamma = -2.66 \pm 0.02$$

$$E_0 = (260 \pm 50) \text{ GeV/n}$$

$$\Delta\gamma = 0.19 \pm 0.04$$

$$\chi^2/\text{dof} = 23/25$$

B fit

$$\gamma = -3.03 \pm 0.03$$

$$E_0 \text{ fixed from C-O}$$

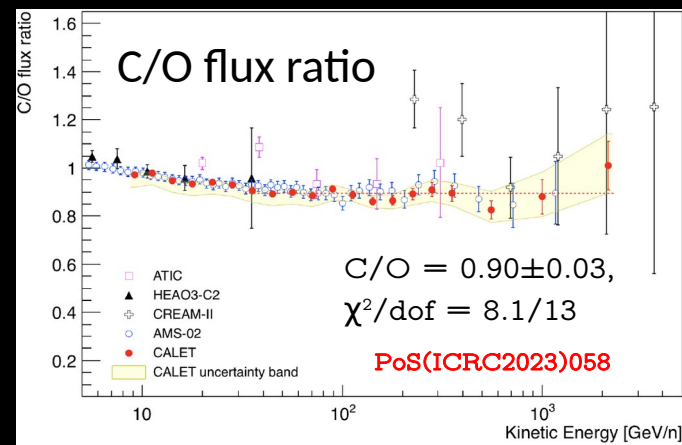
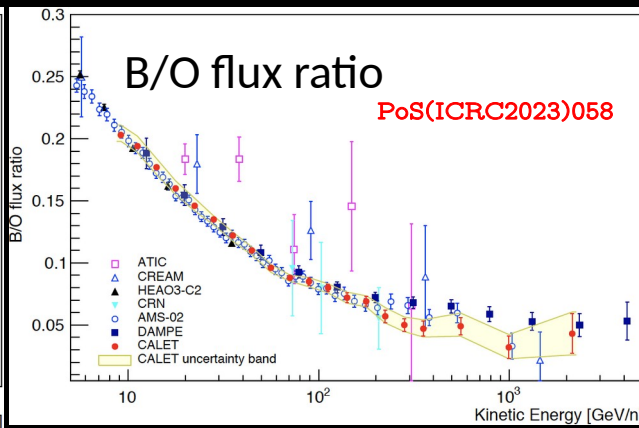
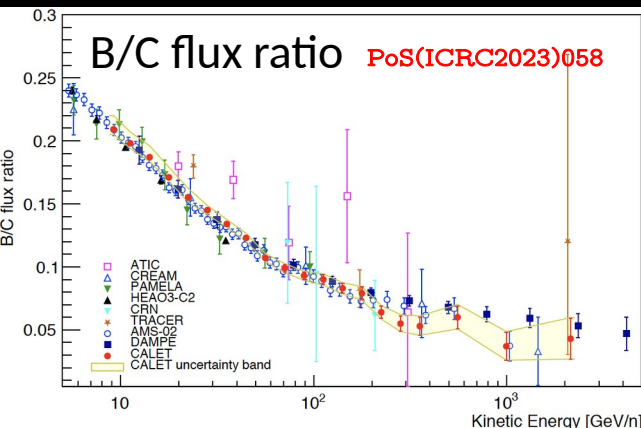
$$\Delta\gamma = 0.32 \pm 0.14$$

$$\chi^2/\text{dof} = 5.2/11$$

Double Power Law

$$\Phi(E) = \begin{cases} c \left(\frac{E}{\text{GeV}}\right)^\gamma & E \leq E_0 \\ c \left(\frac{E}{\text{GeV}}\right)^\gamma \left(\frac{E}{E_0}\right)^{\Delta\gamma} & E > E_0 \end{cases}$$

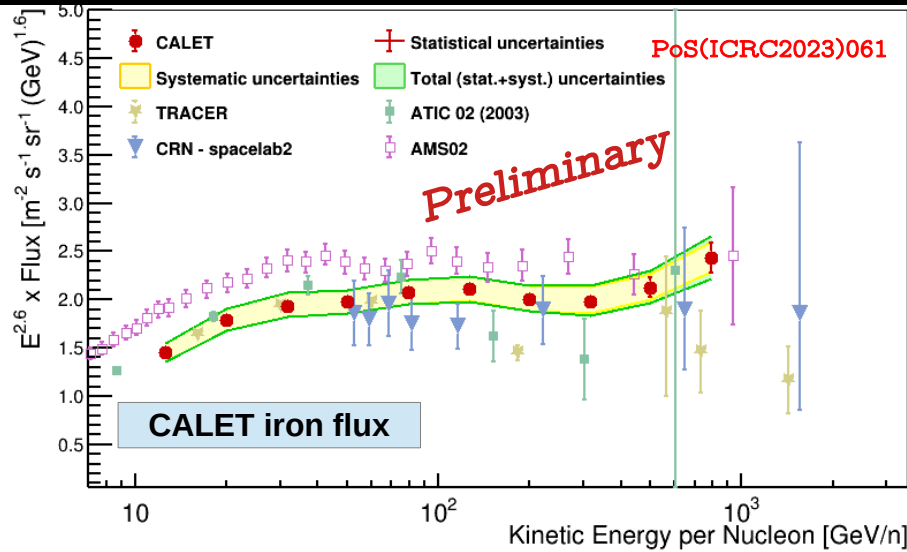
C/O & B/C & B/O ratio



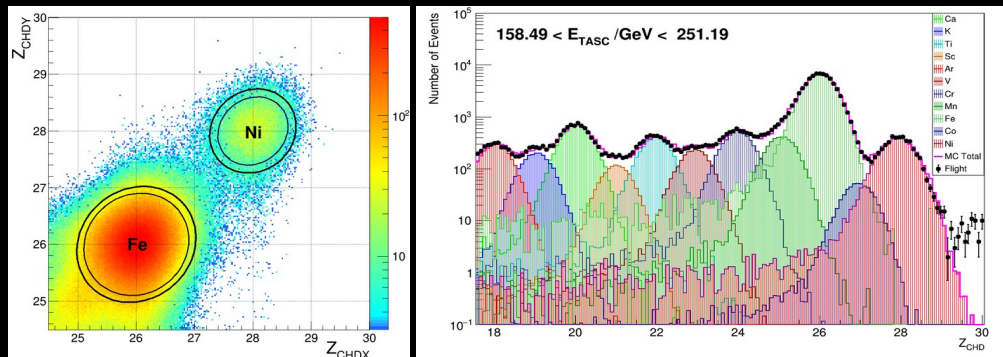
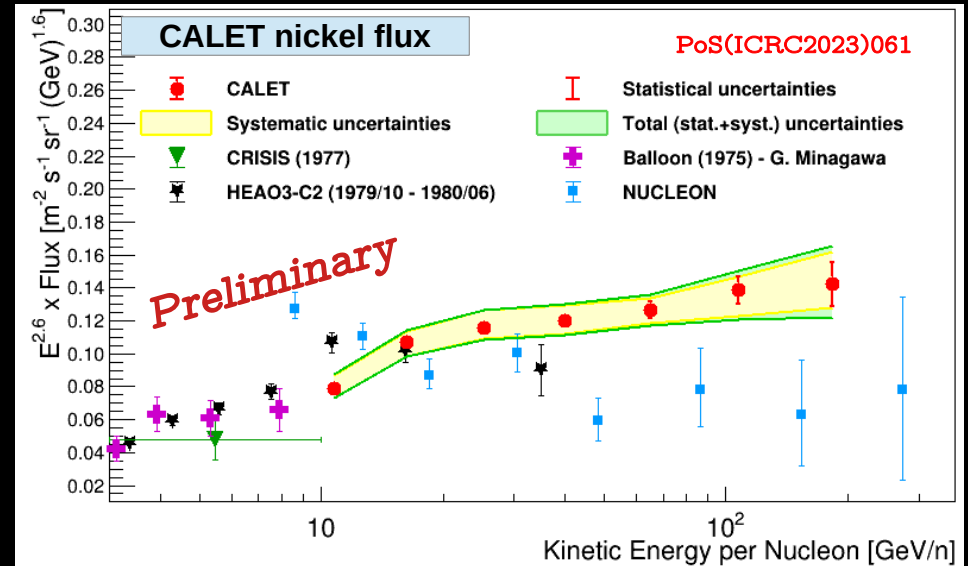
Flux ratios of B/C and B/O are in agreement with AMS02 and lower than DAMPE result above 300 GeV/n, although consistent within the error bars. C/O flux ratio as a function of energy is in good agreement with AMS-02.

- At $E > 30$ GeV/n the C/O ratio is well fitted to a constant value \Rightarrow C and O fluxes have the same energy dependence.
- At $E < 30$ GeV/n C/O ratio is slightly softer \Rightarrow secondary C from O and heavier nuclei spallation

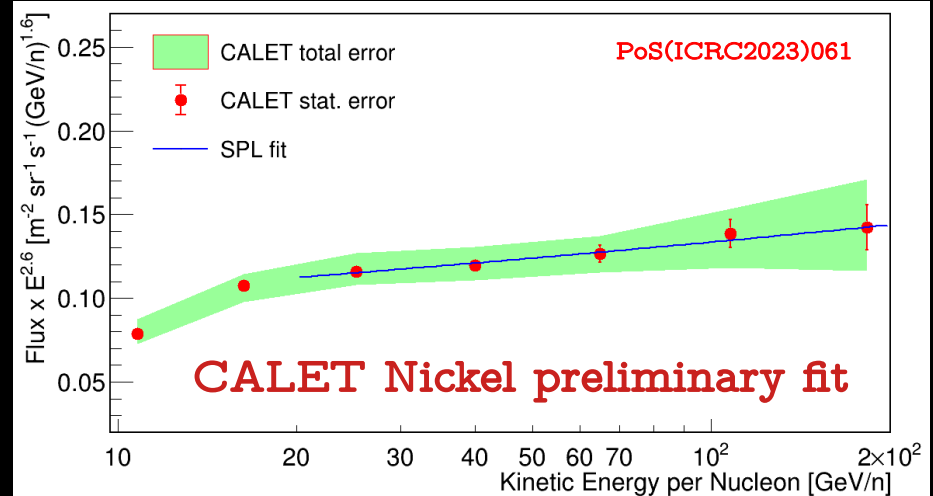
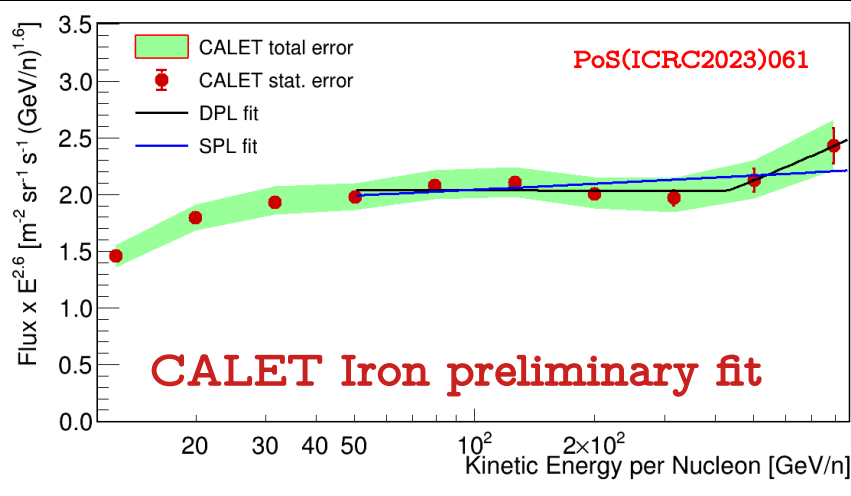
The iron & nickel spectra



- Time period: Nov. 2015 – Dec. 2022
- Iron is consistent within errors with TRACER, ATIC and CRN
- Nickel similar to HEAO3-C2 and NUCLEON though with different spectral shape



The iron and nickel spectral indexes



SPL Fit

$$\Phi(E) = C \left(\frac{E}{1 \text{ GeV}} \right)^\gamma$$

- $\gamma = -2.56 \pm 0.01(\text{stat}) \pm 0.03(\text{sys})$
- $\chi^2/\text{DOF} = 2.7/5$

DPL Fit

$$\Phi(E) = \begin{cases} c \left(\frac{E}{\text{GeV}} \right)^\gamma & E \leq E_0 \\ c \left(\frac{E}{\text{GeV}} \right)^\gamma \left(\frac{E}{E_0} \right)^{\Delta\gamma} & E > E_0 \end{cases}$$

- $\gamma = -2.60 \pm 0.01(\text{stat}) \pm 0.08(\text{sys})$
- $\chi^2/\text{DOF} = 0.8/3$
- $\Delta\gamma = 0.29 \pm 0.27$
- $E_0 = (428 \pm 314) \text{ GeV/n}$

SPL Fit

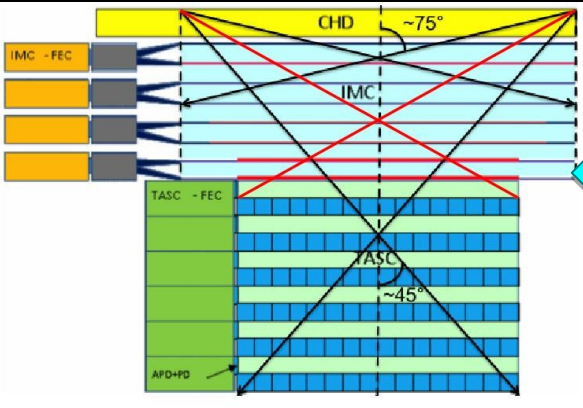
$$\Phi(E) = C \left(\frac{E}{1 \text{ GeV}} \right)^\gamma$$

- $\gamma = -2.49 \pm 0.03(\text{stat}) \pm 0.07(\text{sys})$
- $\chi^2/\text{DOF} = 0.1/3$

The significance of the fit with the DPL in the studied energy range is not sufficient to exclude the possibility of a single power law

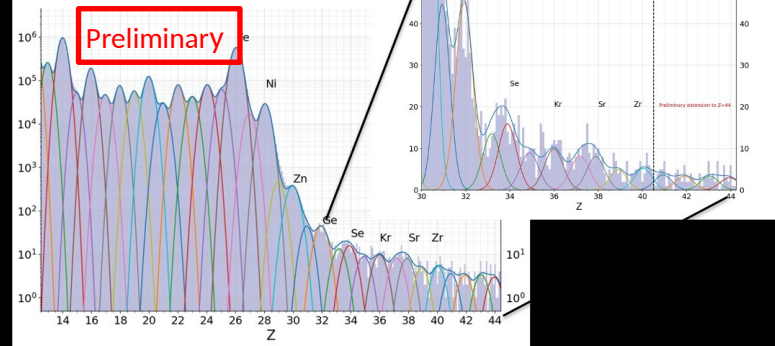
From 20 to 240 GeV/n the nickel flux is consistent with the hypothesis of an SPL Spectrum.

Ultra heavy cosmic ray nuclei

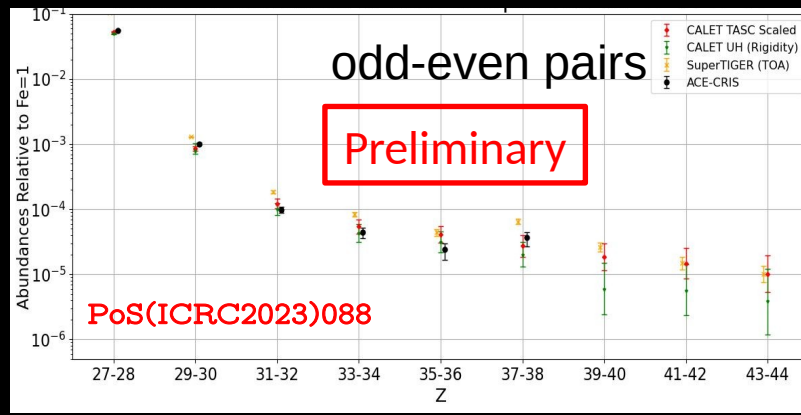
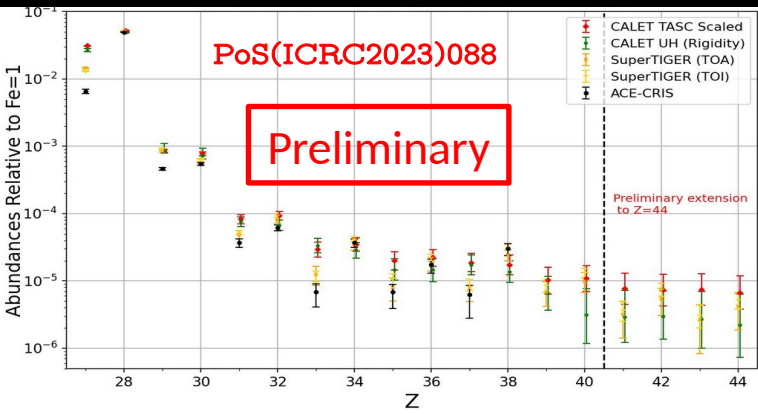


- A special UH CR trigger uses the CHD and the first 4 layers of the IMC to achieve an expanded $\times 4$ geometric factor $GF \sim 4400 \text{ cm}^2 \text{ sr}$ without energy information. (~ 260 million events)
- A subset of events pass through the top of the TASC (~ 65 million events) with energy information.

Charge histogram



Mesurement of the relative abundances of the elements above Fe through ${}_{44}\text{Ru}$ (Fe =1)



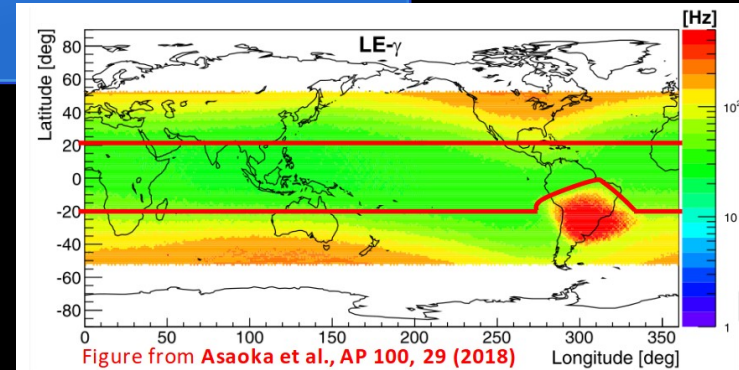
The CALET UH element ratios relative to Fe are consistent with Super-TIGER and ACE abundances.

CALET γ -ray Analysis Overview and GW Follow-up

- Observations with high-energy (HE) trigger are always active ($E > \sim 10$ GeV)
- Observations with low-energy gamma (LEG) trigger are active at low geomagnetic latitudes ($E > \sim 1$ GeV)
- Trigger of CGBM instrument prompts CALET to temporarily activate LEG mode to search for transient counterparts
- Transient analysis pipeline allows for quick follow-up of GRBs or LIGO/Virgo GW triggers

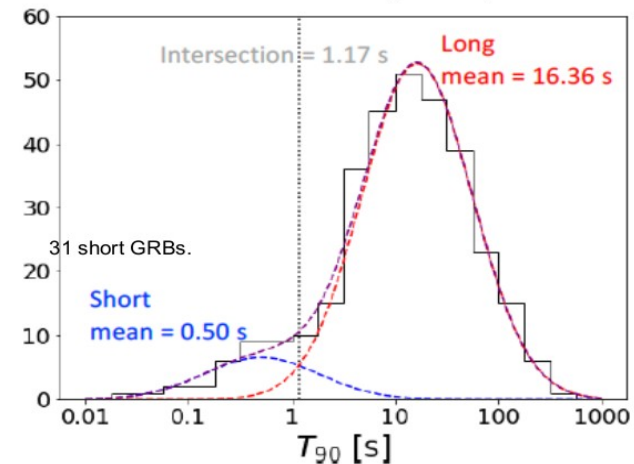
Observations corresponding to triggers in LIGO/Virgo O3-O4 run was analyzed.

No candidate of EM counterparts was found in CALET data. We obtained upper limits of high energy gamma-ray flux



CGBM has detected **327 GRBs** as of June 2023.

Duration distribution measured by SGM (40 – 1000 keV)



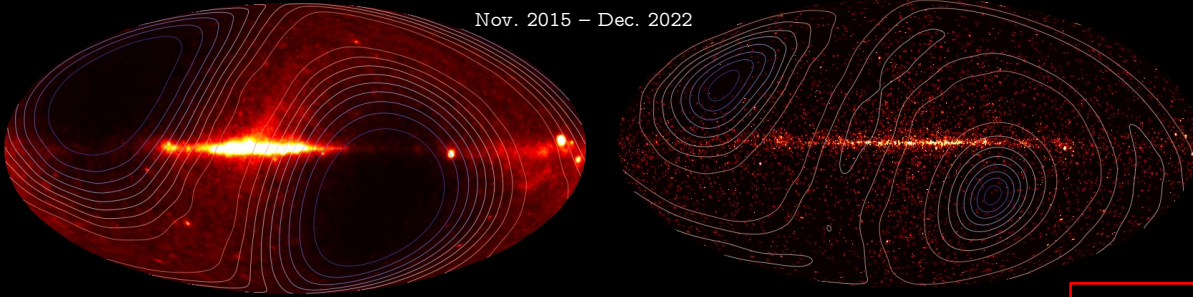
CALET γ -ray Sky Map and Energy Spectra

Effective area: $\sim 400 \text{ cm}^2$ ($>2 \text{ GeV}$)
 Angular resolution: $< 0.2^\circ$ ($> 10 \text{ GeV}$)
 Energy resolution: $\sim 2\%$ ($> 10 \text{ GeV}$)

γ -ray sky map LE- γ trigger ($E > 1 \text{ GeV}$)

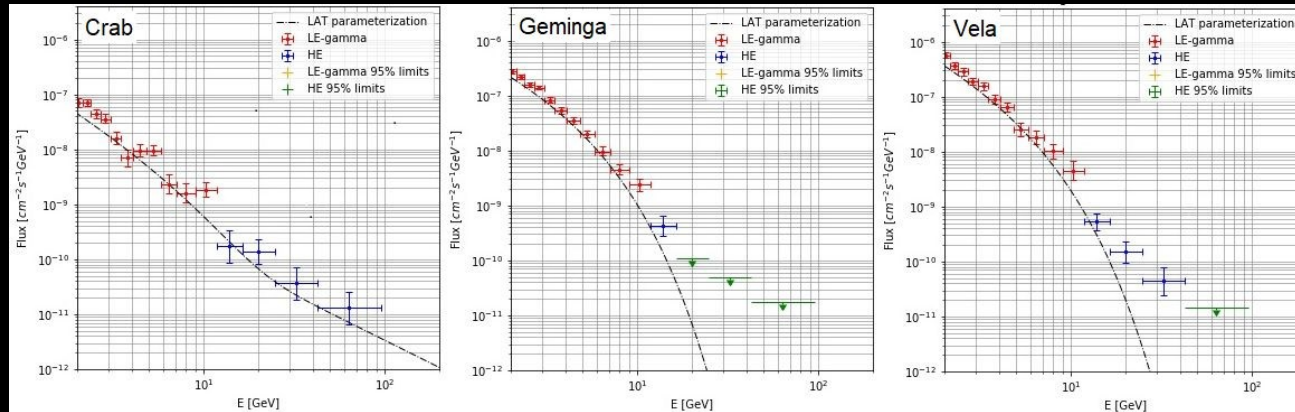
γ -ray sky map HE trigger ($E > 10 \text{ GeV}$)

Nov. 2015 – Dec. 2022



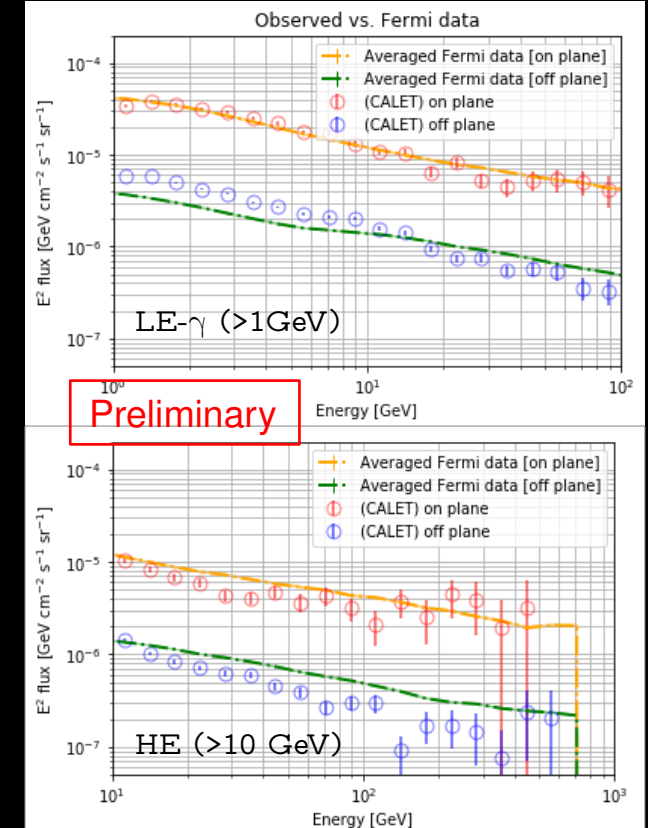
Preliminary

Energy spectra for bright point sources



The spectra for point sources and diffuse components are found to be consistent with those by Fermi-LAT.

Gamma-ray spectrum



Preliminary

"On-plane": $|l| < 80^\circ$ & $|b| < 8^\circ$, "Off-plane": $|b| > 10^\circ$

Solar Modulation and Drift Model

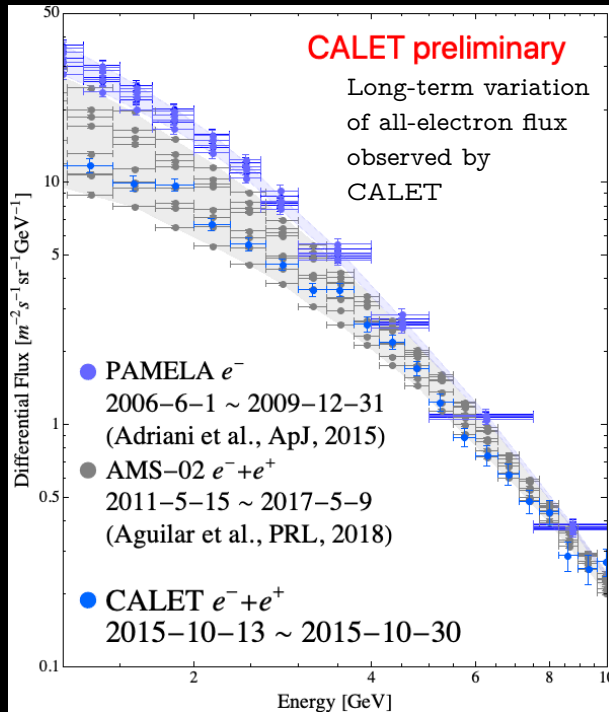
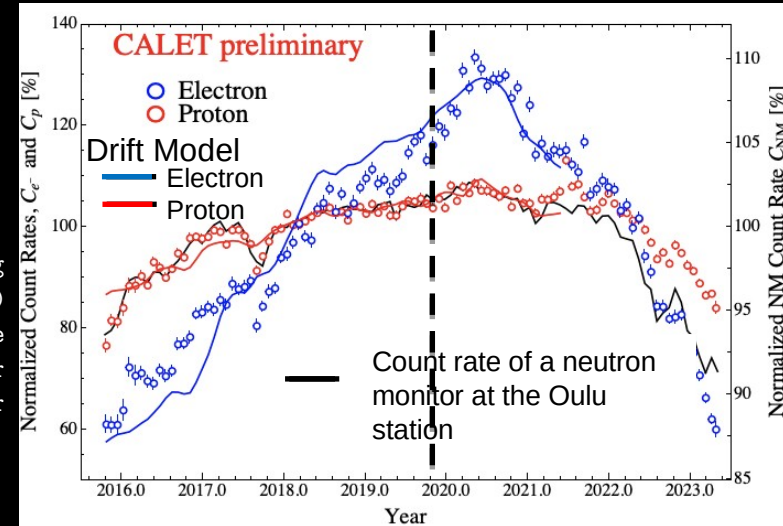
PRL 130 211101 (2023)
& PoS(ICRC2023)1253

24

Since the start of observations in 2015/10, a steady increase in the 1-10 GeV all-electron flux has been observed.

In ~2020, the flux has reached the maximum flux observed with PAMELA during the previous solar minimum.

Solar Modulation during Solar Cycles 24-25 Transition



Good correlation of NM counting rate at Oulu station (black line) with the CR $e^- + e^+$ flux increase in the 1-10 GeV until ~half a year after the beginning the new solar cycle 25.

- We have observed a clear charge-sign dependence of the solar modulation of GCRs, showing that variation amplitude of C_{e^-} is much larger than that of C_p at the same average rigidity.
- We also have succeeded in reproducing variations of C_{e^-} and C_p simultaneously with a numerical drift model of the solar modulation, which implies that the drift effect plays a major role in the long-term modulation of GCRs.
- We also find a clear difference between ratios, C_p/C_{NM} , during the descending phase of the 24th solar cycle and the ascending phase of the 25th solar cycle.

Conclusions

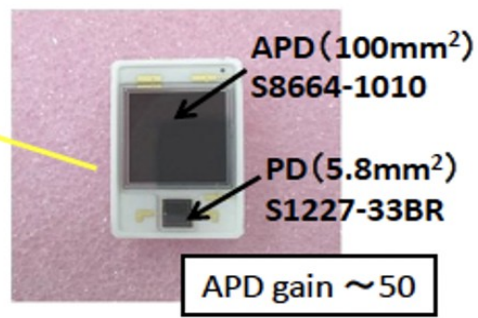
- CALET was successfully launched on Aug. 19th, 2015. The observation campaign started on Oct. 13th, 2015.
- Excellent performance and remarkable stability of the instrument were confirmed.
- CALET obtained precise measurements of the fluxes of CR electrons up to the TeV region, the energy spectra of CR nuclei from proton to nickel up to hundreds of TeV and secondary-to-primary ratios of individual elements:

All-electron spectrum in the range 11 GeV – 7.5 TeV	PRL 131, 191001 (2023)	(3 rd update)
Proton spectrum in the range 50 GeV – 60 TeV	PRL 129, 101102 (2022)	(2 nd update)
Carbon and oxygen spectra in the range 10 GeV/n – 2.2 TeV/n	PRL 125, 251102 (2020)	1 st paper
Iron spectrum in the range 50 GeV/n – 2 TeV/n	PRL 126, 241101 (2021)	1 st paper
Nickel spectrum in the range 8.8 GeV/n – 240 GeV/n	PRL 128, 131103 (2022)	1 st paper
Boron spectrum in the range 8.4 GeV/n – 3.8 TeV/n	PRL 129, 251103 (2022)	1 st paper
Helium spectrum in the range 40 GeV – 250 TeV	PRL 130, 171002 (2023)	new
Preliminary analysis of ultra-heavy cosmic-ray abundances	PoS(ICRC2023)088	preliminary
Solar modulation and drift model	PRL 130, 211001 (2023)	new

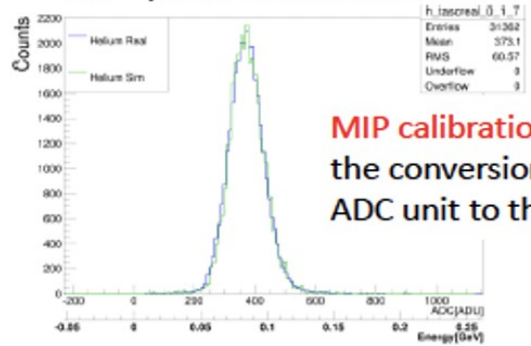
- Analysis of gamma-ray sources and transients continues:
 - GW follow-up and GRB analysis with CGBM & CAL : ApJL 829:L20 (2016)
 - Counterpart search in LIGO/Virgo O3 with CGBM & CAL: ApJ 933:85 (2022)

Extended operations recently approved by JAXA/NASA/ASI through the end of 2030

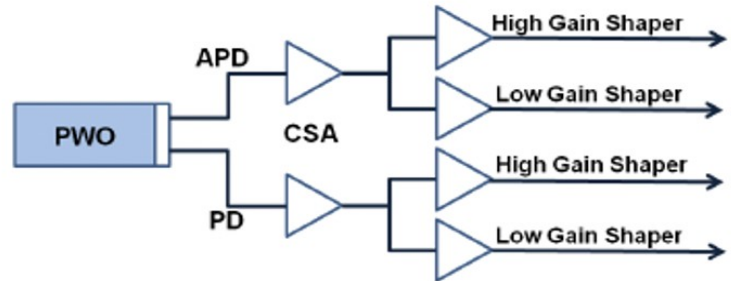
Backup



"MIP" peak in PWO: Obs. vs. MC



MIP calibration determines the conversion factor from ADC unit to the energy

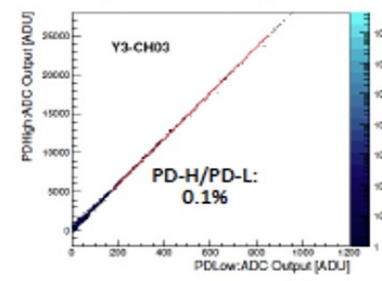
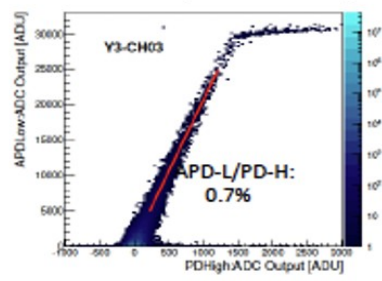
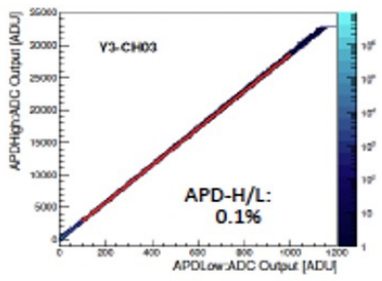


The whole dynamic range was calibrated by UV laser irradiation on ground :
 1) The linearity of each gain range is confirmed in the range of 1.4-2.5 %.
 2) Each channel covers from 1 MIP to 10⁶ MIPs.

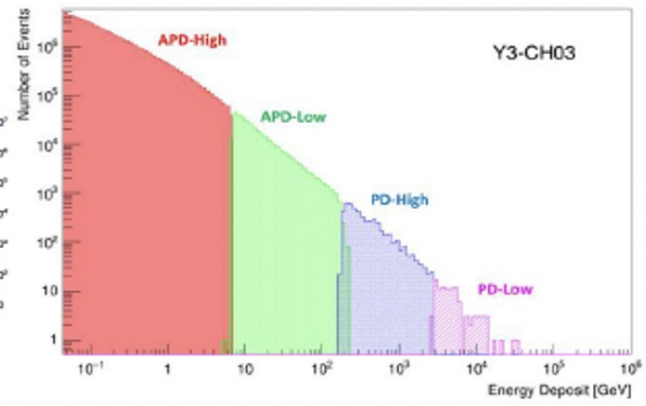
APD-H	APD-L	PD-H	PD-L
1.4%	1.5%	2.5%	2.2%

The correlation between adjacent gain ranges is calibrated by using in-flight data in each channel.

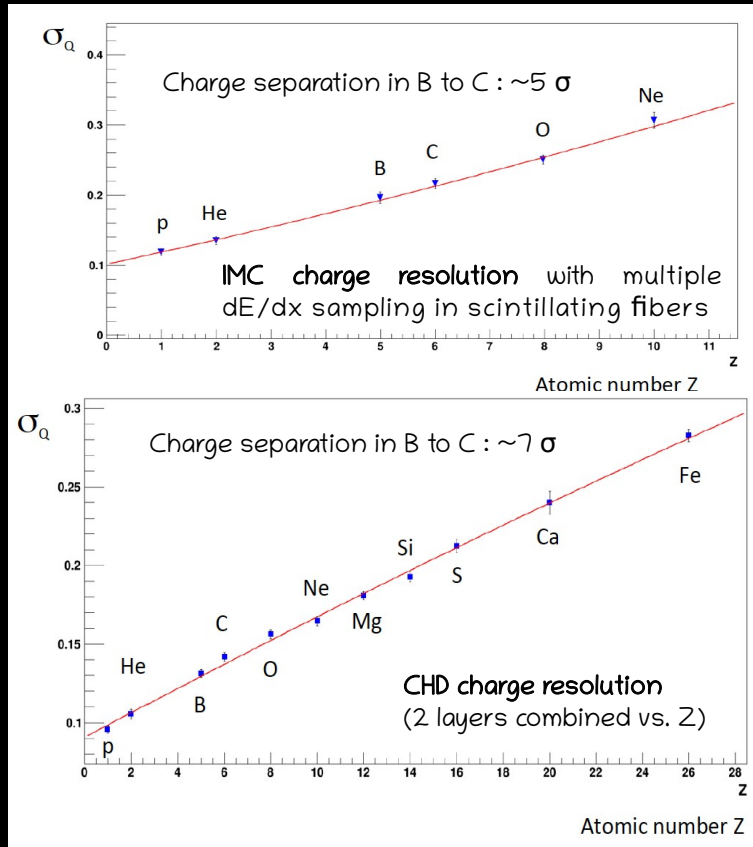
APD-H	APD-L	PD-H
APD-L	PD-H	PD-L
0.1%	0.7%	0.1%



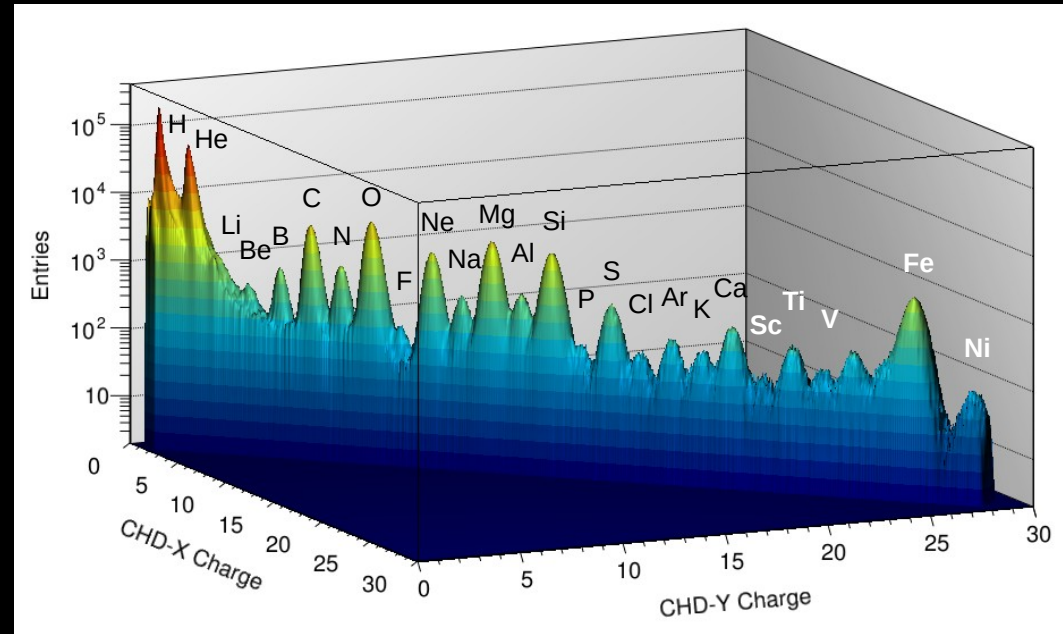
Example of energy distribution in one PWO log



Charge Identification with CALET



- Charge identification for p, He and light nuclei is achieved by CHD+IMC;
- Charge identification for heavy nuclei is achieved by CHD due to saturation of signals occurring in the IMC layers.

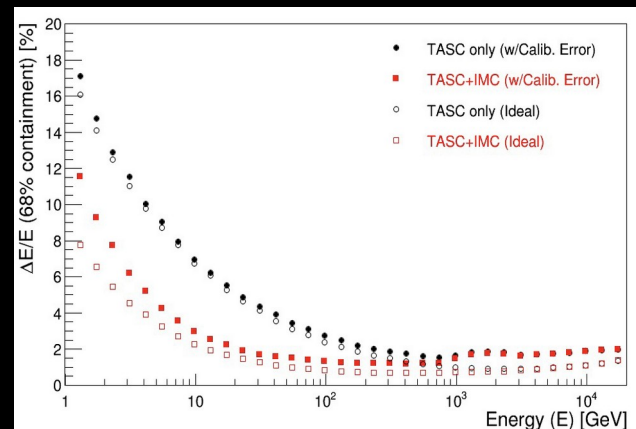
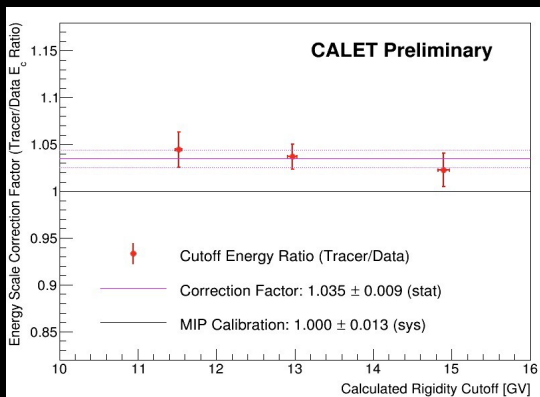


Energy measurement

Electrons

Absolute energy scale calibration for electrons using rigidity cutoff + beam calibration at CERN-SPS

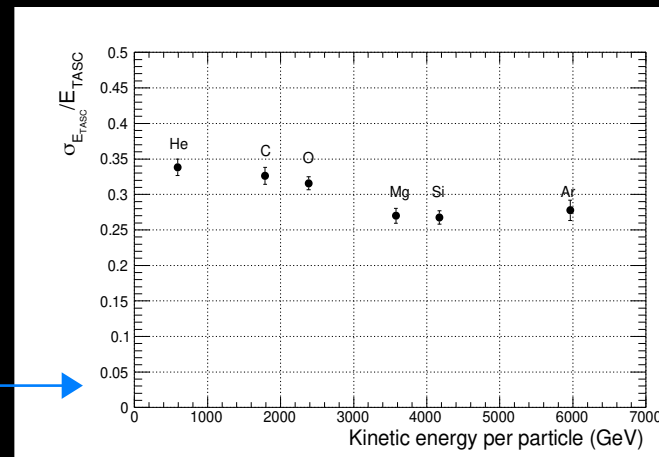
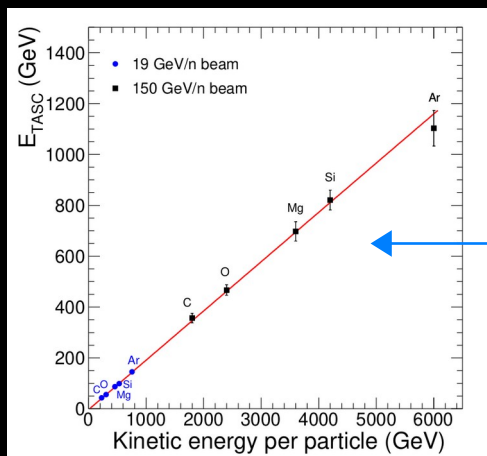
Simulated energy dependence of electron energy resolution:
 < 2% above 20 GeV using both TASC and IMC Including the calibration errors



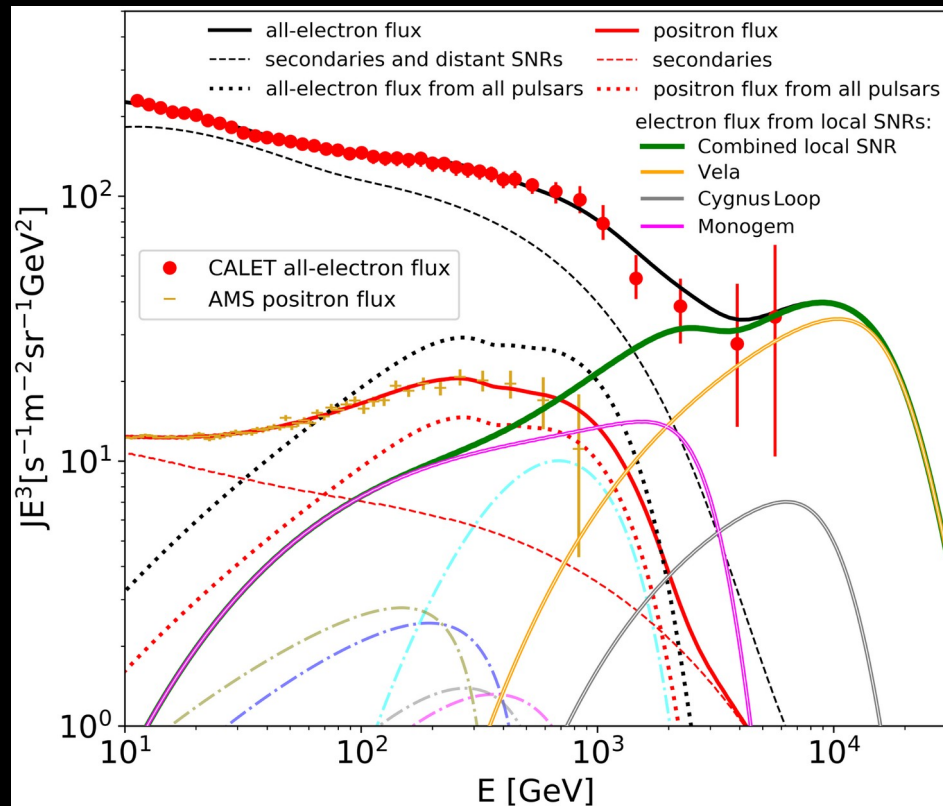
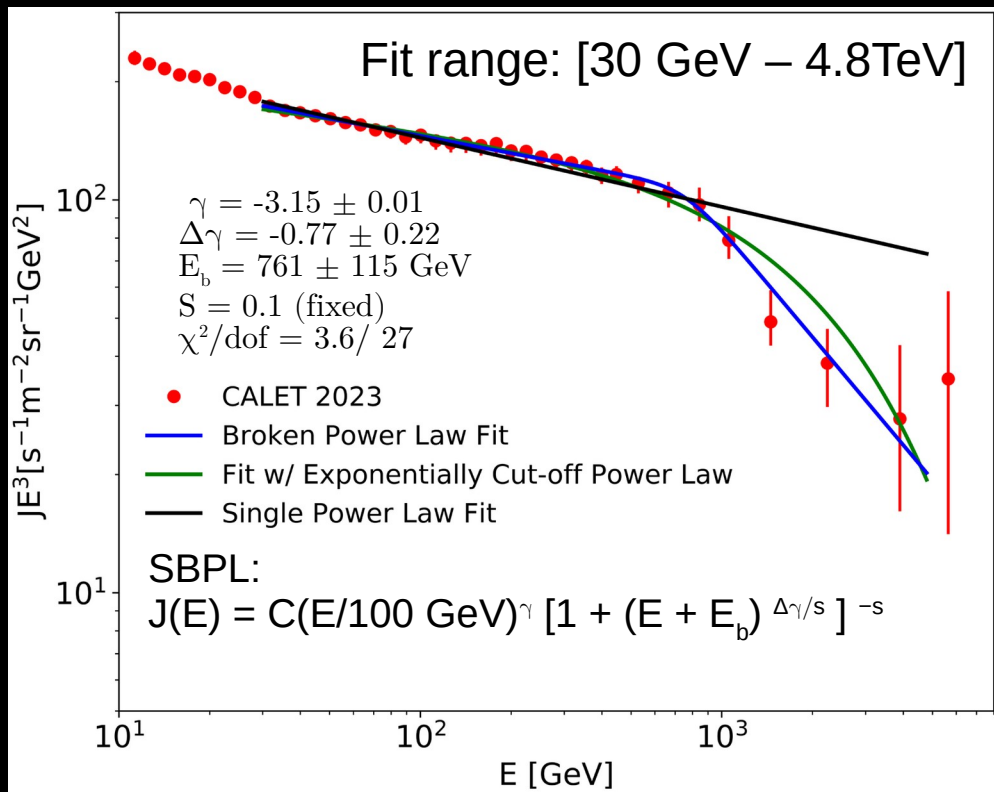
HADRONS

Beam Test Calibration (CERN-SPS in 2015):

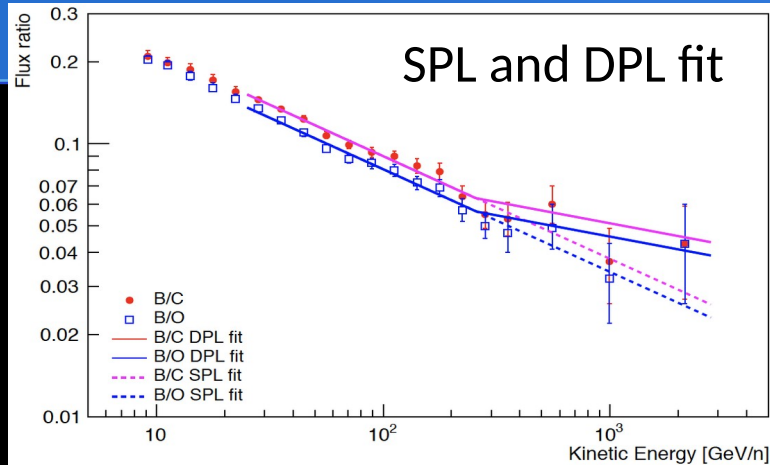
- MC energy tuning with beams of accelerated ion fragments ($A/Z = 2$) of 150 GeV/c/n.
- Good linearity up to maximum available beam energy (~ 6 TeV)
- Fraction of particle energy released in TASC is ~ 20%
- Energy resolution 30-35%



Fit and possible interpretation of CALET all-electron spectrum

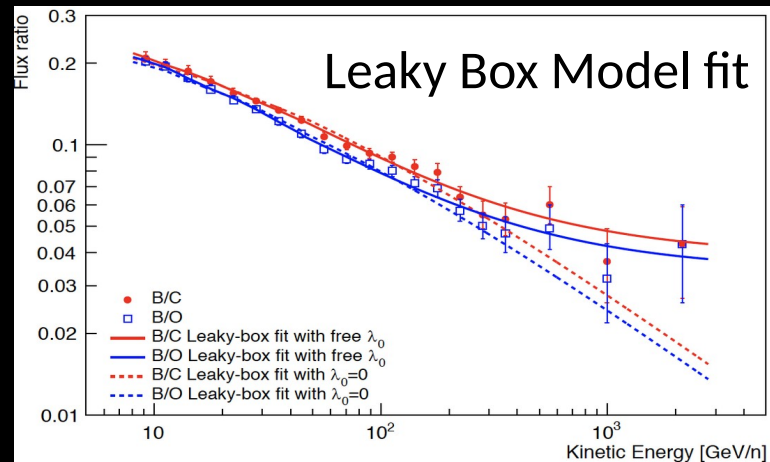


Spectral fit to B/C & B/O ratio



Simultaneous fit to B/C and B/O ($E > 25$ GeV/n) with same parameters except normalization
 SPL fit: $\Gamma = 0.376 \pm 0.014$ ($\chi^2 / \text{dof} = 19/27$)
 DPL fit: $\Delta\Gamma = 0.22 \pm 0.10$ ($\chi^2 / \text{dof} = 15/26$)

Leaky-Box model fit [ApJ 752 69 (2012)]



$$\frac{\Phi_B(E)}{\Phi_C(E)} = \frac{\lambda(E)\lambda_B}{\lambda(E) + \lambda_B} \left[\frac{1}{\lambda_{C \rightarrow B}} + \frac{\Phi_O(E)}{\Phi_C(E)} \frac{1}{\lambda_{O \rightarrow B}} \right]$$

$$\frac{\Phi_B(E)}{\Phi_O(E)} = \frac{\lambda(E)\lambda_B}{\lambda(E) + \lambda_B} \left[\frac{1}{\lambda_{O \rightarrow B}} + \frac{\Phi_C(E)}{\Phi_O(E)} \frac{1}{\lambda_{C \rightarrow B}} \right]$$

$$\lambda(E) = kE^{-\delta} + \lambda_0$$

Fit parameters	$\lambda_0 = 0$ fixed	λ_0 free
k (g/cm ²)	13.1 ± 0.2	13.0 ± 0.3
δ	0.61 ± 0.01	0.81 ± 0.04
l_0 (g/cm ²)	0	1.17 ± 0.16
χ^2 / dof	58.3/38	17.9/37

Significance of $\lambda_0 \neq 0 > 5\sigma$
 \Rightarrow Residual path length could explain the flattening of B/C, B/O ratios at high energies.